

# Accepted Manuscript

Design, synthesis and evaluation of azaacridine derivatives as dual-target EGFR and Src kinase inhibitors for antitumor treatment

Zhishan Cui, Shaopeng Chen, Yanwei Wang, Chunmei Gao, Yuzong Chen, Chunyan Tan, Yuyang Jiang



PII: S0223-5234(17)30367-7

DOI: [10.1016/j.ejmech.2017.05.006](https://doi.org/10.1016/j.ejmech.2017.05.006)

Reference: EJMECH 9436

To appear in: *European Journal of Medicinal Chemistry*

Received Date: 23 December 2016

Revised Date: 28 March 2017

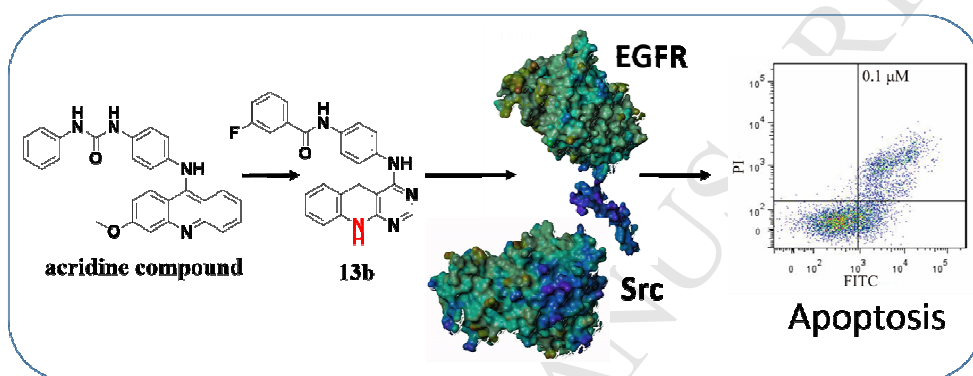
Accepted Date: 2 May 2017

Please cite this article as: Z. Cui, S. Chen, Y. Wang, C. Gao, Y. Chen, C. Tan, Y. Jiang, Design, synthesis and evaluation of azaacridine derivatives as dual-target EGFR and Src kinase inhibitors for antitumor treatment, *European Journal of Medicinal Chemistry* (2017), doi: 10.1016/j.ejmech.2017.05.006.

This is a PDF file of an unedited manuscript that has been accepted for publication. As a service to our customers we are providing this early version of the manuscript. The manuscript will undergo copyediting, typesetting, and review of the resulting proof before it is published in its final form. Please note that during the production process errors may be discovered which could affect the content, and all legal disclaimers that apply to the journal pertain.

## Design, Synthesis and Evaluation of Azaacridine Derivatives as Dual-target EGFR and Src Kinase Inhibitors for Antitumor Treatment

A series of azaacridine compounds were rationally designed and synthesized as EGFR and Src dual inhibitors. The typical compound **13b** could inhibit the invasion of tumor cells and induce cancer cells apoptosis in the nano-molar range.



**Design, Synthesis and Evaluation of Azaacridine Derivatives as Dual-target  
EGFR and Src Kinase Inhibitors for Antitumor Treatment**

Zhishan Cui<sup>a, b†</sup>, Shaopeng Chen<sup>a†</sup>, Yanwei Wang<sup>a, b</sup>, Chunmei Gao<sup>a, b, \*</sup>, Yuzong  
Chen<sup>a, b, c</sup>, Chunyan Tan<sup>a, b</sup>, Yuyang Jiang<sup>a, b, d, \*</sup>

<sup>a</sup> *The Guangdong Province Key Laboratory of Chemical Biology, the Graduate School at Shenzhen, Tsinghua University, Shenzhen 518055, PR China.*

<sup>b</sup> *National & Local United Engineering Lab for Personalized antitumor drugs, the Graduate School at Shenzhen, Tsinghua University, Shenzhen 518055, PR China.*

<sup>c</sup> *Bioinformatics and Drug Design Group, Department of Pharmacy, Centre for Computational Science and Engineering, 117543, Singapore.*

<sup>d</sup> *School of Medicine, Tsinghua University, Beijing 100084, PR China.*

**Keywords**

EGFR; Src; Azaacridine derivatives; Antitumor; Invasion; Apoptosis.

---

\* Corresponding authors. Tel./Fax: +86 (755) 26036533

E-mail: chunmeigao@sz.tsinghua.edu.cn, jiangyy@sz.tsinghua.edu.cn

† Authors with equal contributions.

**Abstract**

Overexpression of EGFR is often associated with advanced stage disease and poor prognosis. In certain cancers, Src works synergistically with EGFR to promote proliferation, survival, invasion and metastasis. Development of dual-target drugs against EGFR and Src is of therapeutic advantage against these cancers. Based on molecular docking and our previous studies, we rationally designed a new series of azaacridine derivatives as potent EGFR and Src dual inhibitors. Most of the synthesized azaacridines displayed good antiproliferative activity against K562 and A549 cells. The representative compound **13b** showed nM IC<sub>50</sub> values against K562 and A549 cells, and inhibited EGFR at inhibition rate of 33.53% at 10 μM and Src at inhibition rate of 72.12% at 1 μM. Furthermore, compound **13b** could inhibit the expression of EGFR, p-EGFR, Src and p-Src. Moreover, **13b** efficiently inhibited the invasion of tumor cells and induced cancer cells apoptosis. Our study suggested that azaacridine scaffold can be developed as novel multi-target kinase inhibitors for cancer therapy.

## 1. Introduction

EGFR (Epidermal Growth Factor Receptor, a class of membrane receptor tyrosine kinases) plays an indispensable role in cancer cell proliferation, survival, adhesion, migration, and differentiation [1-5]. Overexpression of EGFR have been associated with a variety of cancers [6-8]. Development of EGFR inhibitors has become a main focus in antitumor drug campaigns. At present, a series of EGFR inhibitors have been developed, some of which have been approved or entered into clinical phases, such as Gefitinib [9], Erlotinib [10], Icotinib [11], and Lapatinib [12]. However, EGFR signalling pathways involve a complicated network of interconnected circuits. When only EGFR is targeted, redundancy and crosstalk between these pathways will cause drug resistance [13, 14]. Consequently, a huge effort has been poured in the exploration of escape pathways activated by EGFR drugs, which will give more clues for cancer therapy.

Src (sarcoma) is a type of non-receptor tyrosine kinases, which functions in diverse cellular processes [15, 16]. It is an important anticancer target [17], because of its key roles in signalling pathways including apoptosis [18], migration [19] and invasion [20]. Researches showed that the disruption of EGFR and Src interactions could effectively overcome the resistance to EGFR inhibitors in certain cancers [21, 22], for example the combination of Lapatinib and Saracatinib could induce the Lapatinib-resistant cells apoptosis [23]. Therefore, development of drugs targeted both EGFR and Src might offer a better therapeutic advantage. However, to the best of our knowledge, there is no report on the rational design and synthesis of molecules acted as both EGFR and Src dual kinase inhibitors, expect that some drugs targeted EGFR were later found to have Src kinase inhibition activity [24, 25].

Our group has been involved for several years in the design and synthesis of antitumor agents [26-47], including multi-target kinase inhibitors [43-47]. Based on our group previous research and molecular docking methods, we rationally designed a new series of azaacridine derivatives, which can be efficiently bind with the key residues of EGFR and Src. Preliminary *in vitro* antiproliferative ability of synthetic compounds against K562 (a human erythroleukemic cell line) and A549 (a human lung carcinoma cell line) cells were studied, and the structure–activity relationship was disclosed. The mechanism of action of the representative compound **13b** was also studied.

## 2. Results and discussion

### 2.1. Rationale: based on the previous lead and molecular docking method

In the previous paper [43], we reported that the acridine compound (Fig. 1) containing anilinoacridine and phenyl-urea moieties can inhibit the activity of Src, however the inhibition activity need to be improved. We thought that the moderate inhibition activity might be due to the formation of only one hydrogen bond between the acridine compound and the hinge region of Src. Therefore, we converted the scaffold of the acridine compound (the previous lead) to azaacridine, which might form more hydrogen bonds with the hinge region of Src. In addition, we found that azaacridine ring could also bind with the active site of EGFR efficiently. Moreover, amido and urea linkages were also introduced to the azaacridine ring to bind with the DFG-out conformation of Src and the hydrophobic pocket of EGFR, respectively. Therefore, the azaacridine derivatives (Fig. 1) can be potent dual-target EGFR and Src kinase inhibitors.

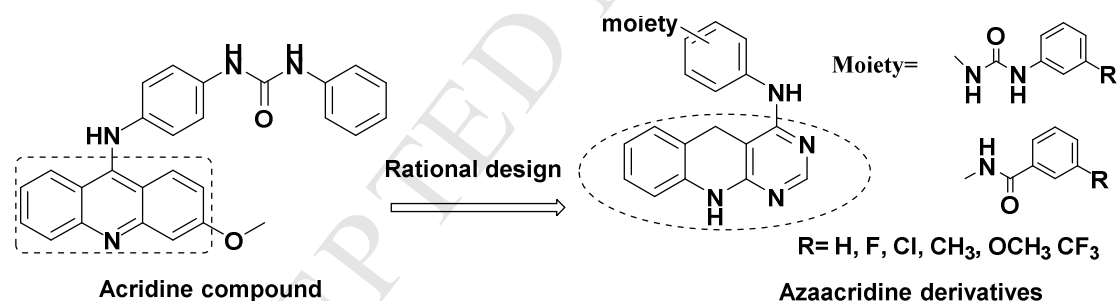


**Fig. 1.** Rational design from the acridine compound to azaacridine derivatives.

Molecular docking confirmed that the azaacridine derivatives had higher binding affinity with EGFR and Src than the acridine compound. The molecular docking study of the representative compound **13b** with EGFR and Src was showed in Fig. 2. For EGFR, the azaacridine ring can form three hydrogen bonds with Thr 766, Gln 767 and Lys 721 in the hinge region area, and the amido linkage can get deep into the hydrophobic pocket region to improve the binding ability. For Src, -NH group and two nitro atoms in the azaacridine ring could form three hydrogen bonds with Met 340, Met 341 and Lys 295. Meanwhile, as we expected, the amido moiety formed two

hydrogen bonds with Glu310 and Asp 404 in the DFG-out pocket. In addition, three  $\pi$ - $\pi$  interaction bonds and one cation- $\pi$  bond were also formed between compound **13b** and Leu 273, Phe 405, Tyr 382, and Lys 295 respectively. The binding energy (CDOCKER Energy and CDOCKER Interaction Energy) had been calculated and showed in Table 1. All the results revealed that the azaacridine derivatives we rationally designed could be potential dual inhibitors of EGFR and Src.

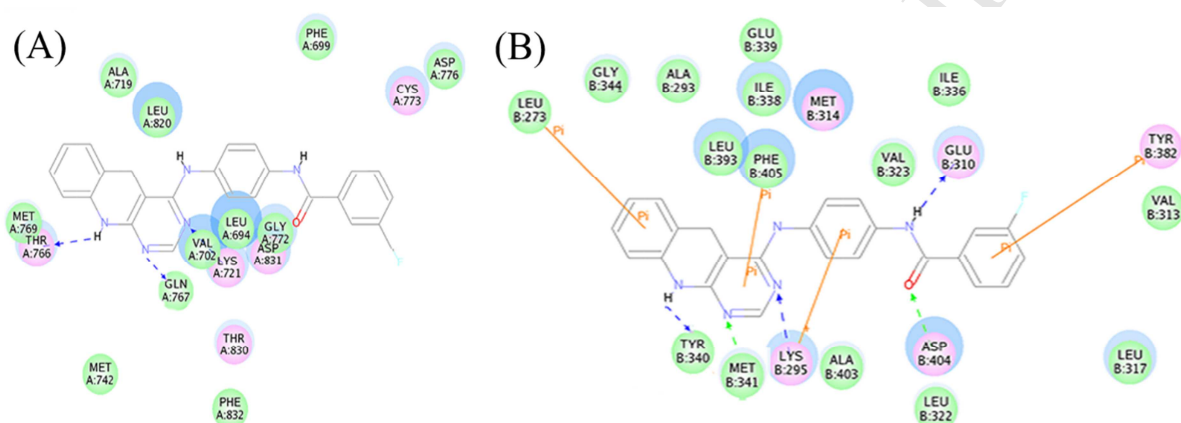


**Fig. 2.** Molecular docking study of **13b** with EGFR and Src. (A) **13b** with EGFR (PDB code 1M17); (B) **13b** with Src(PDB code 3G6H).

**Table 1.** Molecular docking data of the acridine compound and **13b**.

	Src		EGFR	
	Energy <sup>a</sup> (kcal/mol)			
	-CDOCKER	-Interaction	-CDOCKER	-Interaction
<b>Acridine compound</b>	16.96	58.43	18.16	51.34
<b>13b</b>	50.32	62.84	32.27	63.20

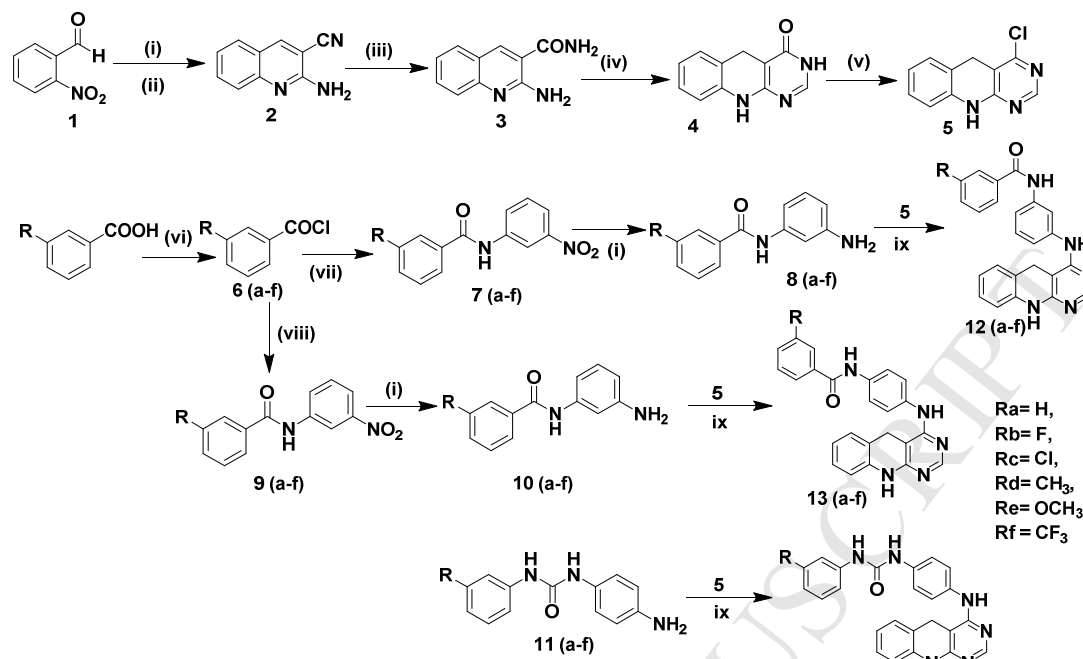
Energy<sup>a</sup>: CDOCKER Energy and CDOCKER Interaction Energy were calculated using Discovery Studio.3.1/CDOCKER Model (EGFR: PDB code 1M17; Src: PDB code 3G6H).

## 2.2. Chemistry

Firstly, a plausible pathway for the synthesis of the intermediate compound **5** was proposed in Scheme 1. The reduction reaction of nitrobenzaldehyde **1** with Fe and NH<sub>4</sub>Cl was carried out in EtOH/H<sub>2</sub>O, which was further reacted with malononitrile to obtain compound **2** in good yield. Hydrolysis of **2** gave compound **3**. Cyclization of compound **3** with formamide got compound **4**. As compound **4** was important, the reaction conditions were optimized, and the yield reached up to 85% (Table 1s). Chlorination of compound **4** by POCl<sub>3</sub> obtained compound **5** in good yield (80%), the structure of which was confirmed by <sup>1</sup>H NMR, <sup>13</sup>C NMR, DEPT135, <sup>1</sup>H-<sup>1</sup>H COSY and HSQC (Fig. 1s).

Secondly, the side chains were synthesized. The synthesis of amide linkers was illustrated in Scheme 1. Different substituents of benzoic acid were treated with SOCl<sub>2</sub> to get compounds **6 (a-f)**, which were then reacted with 3-nitroaniline or *p*-nitroaniline to obtain compounds **7 (a-f)** and **9 (a-f)**, respectively. Subsequent reduction of **7 (a-f)** and **9 (a-f)** in the presence of Fe and NH<sub>4</sub>Cl led to the expected amide derivatives **8 (a-f)** and **10 (a-f)**. The phenyl-urea linker **11 (a-f)** were synthesized according to our early paper[43].

Lastly, the nucleophilic substitution reaction was carried out between compound **5** and the side chains **8 (a-f)**, **10 (a-f)** and **11 (a-f)** to obtain the desired compounds **12 (a-f)**, **13 (a-f)**, and **14 (a-f)** in moderate to good yields.



**Scheme 1.** Synthetic pathway to prepare the target compounds **12 (a-f)**, **13 (a-f)**, **14 (a-f)**. Reagents and conditions: (i) Fe, NH<sub>4</sub>Cl, reflux, 2 h; (ii) malononitrile, 85 °C, 3 h; (iii) conc. H<sub>2</sub>SO<sub>4</sub>, r.t., 24 h; (iv) formamide, 160 °C 12 h; (v) POCl<sub>3</sub>, 100 °C, 3 h; (vi) SOCl<sub>2</sub>, 80 °C, 2-3 h; (vii) 3-nitroaniline, CH<sub>2</sub>Cl<sub>2</sub>, -20 °C, r.t., 2 h; (viii) *p*-nitroaniline, CH<sub>2</sub>Cl<sub>2</sub>, -20 °C, r.t., 2 h; (ix) isopropanol, Et<sub>3</sub>N, reflux, overnight.

### 2.3. *In vitro* cell growth inhibition assay

The antiproliferative activity of the desired azaacridine derivatives was tested against K562 and A549 cells by MTT assay, the acridine compound and Imatinib were used as the positive controls. As shown in Table 2, most of the compounds displayed good antiproliferative activity against K562 with low micromolar IC<sub>50</sub> values, and both the position of the amide-/urea linker in the phenyl ring and the substituents affected the antiproliferative activity significantly. As the synthesized compounds were more sensitive to K562 cells than A549 cells, K562 cells were selected to study the structure-activity relationship (Fig. 3).

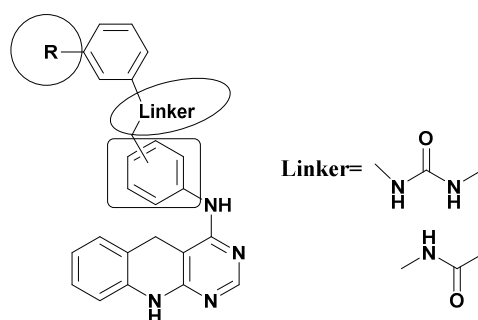


**Fig. 3.** The structure of azaacridine derivatives.

Firstly, the substituents (R) played a significant role in the antiproliferative activity. As showed in Table 2, the introduction of fluorine group can increase the antiproliferative activity greatly (**12b** : 0.72  $\mu\text{M}$  vs **12a** : 3.11  $\mu\text{M}$ , **13b** : 0.22  $\mu\text{M}$  vs **13a** : 2.52  $\mu\text{M}$ , **14b** : 3.14  $\mu\text{M}$  vs **14a** : 5.08  $\mu\text{M}$ ), and compound **13b** exhibited the most cytotoxic activity with an  $\text{IC}_{50}$  value of 0.22  $\mu\text{M}$ , which was better than the acridine compound and Imatinib. When the substituent was a chlorine group, the cytotoxicity was also increased (**12c** : 1.21  $\mu\text{M}$  vs **12a** : 3.11  $\mu\text{M}$ , **13c** : 0.41  $\mu\text{M}$  vs **13a** : 2.52  $\mu\text{M}$ , **14c** : 3.08  $\mu\text{M}$  vs **14a** : 5.08  $\mu\text{M}$ ), however, they were less potent than fluorine substituted compounds (except **14c** : 3.08  $\mu\text{M}$ ). The tri-fluoromethyl group was also a good choice. Compounds **12f** (1.89  $\mu\text{M}$ ), **13f** (1.32  $\mu\text{M}$ ) and **14f** (3.35  $\mu\text{M}$ ) also displayed better antiproliferative activity than compounds **12a** (3.11  $\mu\text{M}$ ), **13a** (2.52  $\mu\text{M}$ ) and **14a** (5.08  $\mu\text{M}$ ), respectively.

**Table 2.** Anti-proliferation activities against K562 and A549 cells of the designed compounds **12 (a-f)**, **13 (a-f)** and **14 (a-f)**.

Entry	Compound	R	$\text{IC}_{50}(\mu\text{M})$	
			K562	A549
1	<b>12a</b>	H	3.11±0.39	18.29±0.22
2	<b>12b</b>	F	0.72±0.16	9.05±0.51

3	<b>12c</b>	Cl	1.21±0.32	12.32±0.19
4	<b>12d</b>	Me	4.90±0.12	>25
5	<b>12e</b>	OMe	3.08±0.57	13.46±1.23
6	<b>12f</b>	CF <sub>3</sub>	1.89±0.38	9.58±0.67
7	<b>13a</b>	H	2.52±0.14	14.29±0.72
8	<b>13b</b>	F	0.22±0.03	0.253±0.16
9	<b>13c</b>	Cl	0.41±0.16	20.69±1.29
10	<b>13d</b>	Me	3.62±0.24	24.77±1.08
11	<b>13e</b>	OMe	2.16±0.01	14.07±0.67
12	<b>13f</b>	CF <sub>3</sub>	1.32±0.01	12.25±0.03
13	<b>14a</b>	H	5.08±0.11	18.01±1.27
14	<b>14b</b>	F	3.14±0.06	6.82±1.42
15	<b>14c</b>	Cl	3.08±0.29	17.93±0.79
16	<b>14d</b>	Me	6.97±0.37	>25
17	<b>14e</b>	OMe	3.62±0.35	13.42±0.2
18	<b>14f</b>	CF <sub>3</sub>	3.35±0.09	9.26±0.67
19	<b>Acridine compound</b>		4.08±0.14	9.03±0.11
20	<b>Imatinib</b>	-	0.53±0.01	4.56±0.23

The introduction of methoxyl group almost had no effect on the antiproliferative activity compared to the corresponding compounds with no substituents (**12e** : 3.08  $\mu$ M vs **12a** : 3.11  $\mu$ M, **13e** : 2.16  $\mu$ M vs **13a** : 2.52  $\mu$ M, **14e** : 3.62  $\mu$ M vs **14a** : 5.08  $\mu$ M). However, when changing methoxyl to methyl group, compounds showed decreasing inhibitory effect (**12d** : 4.90  $\mu$ M vs **12a** : 3.11  $\mu$ M, **13d** : 3.62  $\mu$ M vs **13a** : 2.52  $\mu$ M, **14d** : 6.97  $\mu$ M vs **14a** : 5.08  $\mu$ M).

Secondly, the position of the amide linker had some effect on the antiproliferative activity. Compared with the data in Table 2, compounds **13** with amide bond linker at para-position had higher cytotoxicity activity than compounds **12** generally. Thirdly, the influence of linkers on the antiproliferation activity was also discussed. As amide

bond and urea are the most commonly used linkers, compounds **13 (a-f)** and **14 (a-f)** bearing amide and urea linkers at para-position in phenyl ring were synthesized. In Table 2, compounds **13** almost had better inhibitory effect than compounds **14**, which indicated the amide linker was better than the corresponding urea linker. These results above suggested that the substituents, the linker and its position in phenyl ring could change the cytotoxic profile.

#### 2.4. Inhibition assay

As the designed compounds had good antiproliferative activity, *in vitro* EGFR and Src kinase inhibition capability was firstly evaluated to see whether their cytotoxicity was due to kinase inhibition. As shown in Table 3, almost all the compounds displayed better Src inhibition activity than the acridine compound, except **14c** and **14f**, which showed comparable Src inhibition activity with the acridine compound at 10  $\mu\text{M}$ . In addition, compound **13b** inhibited 72.12% of Src activity at 1  $\mu\text{M}$ . At the same condition, 17 compounds exhibited moderate activity against EGFR at 10  $\mu\text{M}$  (Table 3), except that compound **13f** had 95.41% and 52.38% inhibition rates against EGFR at 10  $\mu\text{M}$  and 1  $\mu\text{M}$ , respectively. As compound **13b** displayed the lowest  $\text{IC}_{50}$  values against both K562 and A549 cells, as well as good Src and moderate EGFR inhibition capability, it was selected as a representative compound to do further studies.

To further evaluate whether EGFR and Src are the targets, we evaluated the influences of **13b** on the expression levels of EGFR, p-EGFR, Src and p-Src in A549 cells. After a 48 h treatment with **13b** at four concentrations (0, 0.1, 0.5, and 2.5  $\mu\text{M}$ ), A549 cells were harvested and lysed for an IP/wt assay. As shown in Fig. 4, compound **13b** inhibited the protein expression levels of EGFR, p-EGFR, Src and p-Src in a dose-dependent manner. Compared with the control, the expression level of EGFR and p-EGFR experienced a sharp decline from 48.02% to 3.03% and 50.21% to 3.11% with the concentration of **13b** increased from 0.1  $\mu\text{M}$  to 2.5  $\mu\text{M}$ , respectively. The same trend was also

observed in the expression of Src and p-Src. Therefore, it is reasonable to conclude that inhibition of EGFR and Src is the main cause for the high antiproliferation activity of compound **13b**.

**Table 3.** Inhibition test of 18 compounds against EGFR and Src.

Entry	Compound	R	Inhibition rate (%)	
			EGFR	Src
1	<b>12a</b>	H	30.70	75.63
2	<b>12b</b>	F	24.50	69.91
3	<b>12c</b>	Cl	30.25	79.23
4	<b>12d</b>	Me	52.99	72.03
5	<b>12e</b>	OMe	31.85	86.86
6	<b>12f</b>	CF <sub>3</sub>	16.31	72.88
7	<b>13a</b>	H	12.56	66.31
8	<b>13b</b>	F	33.15	75.42
9	<b>13c</b>	Cl	30.93	77.54
10	<b>13d</b>	Me	51.07	60.38
11	<b>13e</b>	OMe	35.38	88.77
12	<b>13f</b>	CF <sub>3</sub>	95.41	76.69
13	<b>14a</b>	H	32.01	73.09
14	<b>14b</b>	F	55.36	79.87
15	<b>14c</b>	Cl	42.11	59.11
16	<b>14d</b>	Me	65.39	66.10
17	<b>14e</b>	OMe	24.89	86.01
18	<b>14f</b>	CF <sub>3</sub>	35.38	53.38
19	<b>Acridine compound</b>	-	21.39	59.67
20	<b>Imatinib</b>	-	-	97.12

Moreover, DNA binding assay was also evaluated, as acridine derivatives generally have good DNA binding ability. UV-vis spectrophotometric titration experiments indicated that the DNA binding ability of **13b** was very weak compared with our synthesized DNA binding agents [48, 49], which indicated that DNA binding was not the main reason for the antiproliferative activity of compound **13b** (Fig. 2s). The spectrofluorimetric study was also performed to further evaluate the DNA binding ability of **13b**, and the quenching constant was  $973.23 \text{ M}^{-1}$  (Fig. 2s), which was about 100-fold lower than the DNA binding agents with similar antiproliferative activity published by our group [26, 31, 32, 36]. All the results indicated that DNA was not contribute to the cytotoxicity, and EGFR and Src were the targets of compound **13b**. Although the kinases activities of synthesized compounds were weaker than the antiproliferative activity, the synergistic effects of multi-target agents of moderate activities might contribute to the cytotoxicity [50].

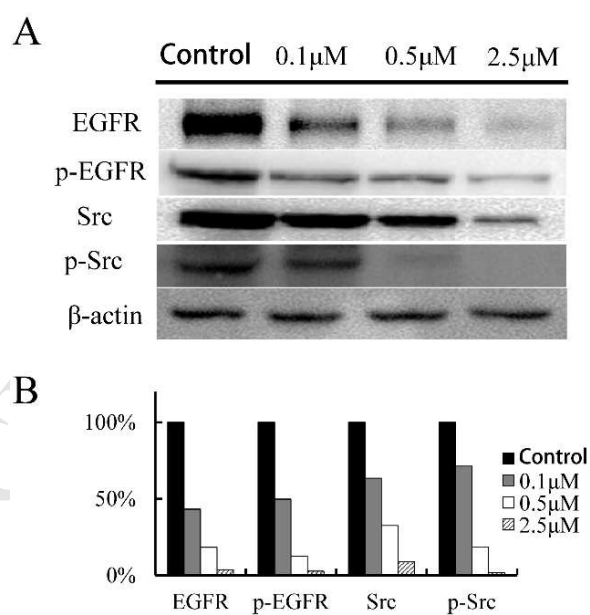


**Fig. 4.** Western blot analysis of **13b**. (A) The inhibition effects of compound **13b** (0.1  $\mu\text{M}$ , 0.5  $\mu\text{M}$  and 2.5  $\mu\text{M}$ ) on the expression of EGFR, p-EGFR, Src and p-Src in A549 cells are depicted. Equal loading was testified by the detection of  $\beta$ -actin. (B) The percentages of protein expressions in the different concentrations of compound **13b**.

### 2.5. Effects of compound **13b** on invasion

As Src plays an important role in cancer invasion, the effects of compound **13b** on A549 cell invasion were assessed using transwell assays, in which the number of invading cells reflected the invasive capacity of the cells. Results in Fig. 5A showed after treatment of compound **13b**, the invasion of A549 cells was inhibited. As depicted in Fig. 5B, compared with the control, compound **13b** at 0.1  $\mu\text{M}$  and 1  $\mu\text{M}$  potently produced rates of inhibition of 52.50% and 82.81%, respectively. These results demonstrated that **13b** could efficiently inhibit the invasion of tumor cells.

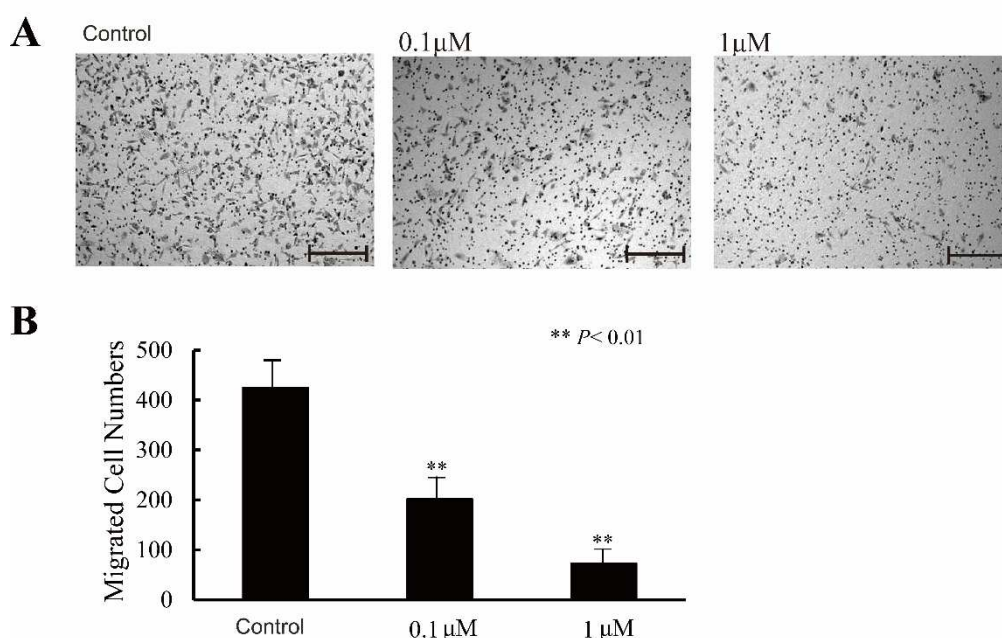


**Fig. 5.** Transwell assay of **13b**. (A) Images depicting the penetration of A549 cells through the filter membrane, 200  $\mu\text{M}$  bar. (B) The number of A549 cells that penetrated the membrane was quantified by Image-Pro-Plus 6.0 of Media Cybernetics (MD, USA). Data are represented as the mean  $\pm$  SEM of five different experiments: \*\*( $p < 0.01$ ) versus control.

### 2.6. Apoptosis induced by compound **13b**

EGFR and Src inhibitors can induce cancer cell apoptosis. Due to **13b** could inhibit EGFR and Src activity and displayed good antiproliferative activity, it was selected to

test its impact on apoptosis. Compound **13b** induced K562 cells apoptosis in a concentration-dependent manner (Fig. 6). The early apoptosis ratio increased from 4.68% to 18.82% with increasing **13b** concentration from 0  $\mu\text{M}$  to 0.1  $\mu\text{M}$ , when compound **13b** was added in K562 cells for 48 h. As the concentration of **13b** increased from 0.1  $\mu\text{M}$  to 1  $\mu\text{M}$ , more and more apoptotic cells progressed from the early stage to the late stage resulting in either death or secondary necrosis. The results indicated that compound **13b** could effectively induce K562 cells apoptosis.

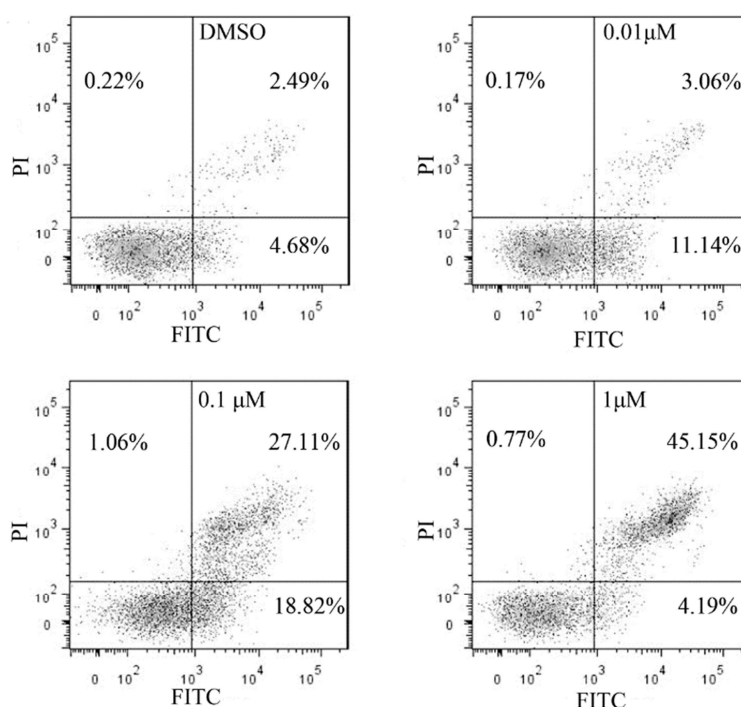


**Fig. 6.** Apoptosis assay of **13b**. Analysis was carried out on a flow cytometer using an Annexin V-FITC/PI apoptosis staining kit according to the manufacturer's instructions.

### 3. Conclusion

To summarize, we designed and synthesized a new series of azaacridine derivatives as potent EGFR and Src dual inhibitors. The results showed that most of the synthesized azaacridine compounds possessed good antiproliferative activity against K562 and A549 cells. The representative **13b** could inhibit the activity of EGFR and Src, inhibit the invasion of tumor cells and induce tumor cell apoptosis. Further

optimization of this structure for improved the kinase inhibition activity and antiproliferative activity is ongoing.

#### 4. Experimental section

##### 4.1. Chemistry

Generally, the procedure for the synthesis of **5** was as follows. Nitrobenzaldehyde **1** (10 mmol) was added to EtOH/H<sub>2</sub>O (25 mL/5 mL) at room temperature, followed by Fe (3.0 equiv) and NH<sub>4</sub>Cl (1.0 equiv). The resultant mixture was heated to reflux and stirred for 2 h. And then, the hot liquid was filtrated rapidly through celite. The appropriate malononitrile (1.0 equiv) and EtOH (10 mL) were added to the filtrate and stirred at 80 °C for 4 h. Then, the mixture was cooled to room temperature and the formed precipitates were filtered off. Washed the precipitates with diethyl ether, we obtained the pure compound **2**. At room temperature, compound **2** (10 mmol) was dissolved in conc. H<sub>2</sub>SO<sub>4</sub> (8 mL) and then stirred for 24 h. The liquid was poured into ice water (80 mL), and NaOH (2 mol/L, aq) as the neutralizer was used to deal with the redundant conc. H<sub>2</sub>SO<sub>4</sub>. Filtered the precipitates, the filter cake was washed with water and dried under vacuum to obtain **3** (yield, 95%). Cyclization of compound **3** (10 mmol) with formamide (10 mL) at 160 °C for 12 h under air, we got compound **4** through filtration and washing with MeOH (15 mL) (yield, 85%). POCl<sub>3</sub> (5 mL) was added to compound **4** (10 mmol) and stirred at 80 °C for 3 h. Cooled the solution and poured into ice water (100 mL), we titrated with NaOH (2 mol/L, aq) in the mixture solution till pH = 8. Filtered the precipitates, the filter cake was washed with water and dried under vacuum to obtain the compound **5** in high yield (80%).

Generally, the procedure for the synthesis of **12-14 (a-f)** was as follows. Compounds **8 (a-f)** (0.41 mmol) and compound **5** (0.4 mmol) were dissolved in isopropanol (10 mL) in the presence of Et<sub>3</sub>N (1 mL). The mixture was stirred for overnight at 80 °C. The raw products were filtered off, washed with diethyl ether to obtain the desired pure compounds **12 (a-f)** in moderate to good yields. Those crude products were purified by column chromatography with CH<sub>2</sub>Cl<sub>2</sub> and MeOH (50:1

v/v). The same processes were used to get the compound **13 (a-f)** and compound **14 (a-f)**.

4.1.1. N-(3-((5,10-dihydropyrimido[4,5-b]quinolin-4-yl)amino)phenyl)-benzamide (**12a**). Yellow solid; yield, 83.7%; mp, 218.2-219.0 °C; <sup>1</sup>H NMR (400 MHz, DMSO-*d*<sub>6</sub>) δ 10.19 (s, 1H), 9.76 (s, 1H), 8.25 (s, 1H), 7.76-7.71 (m, 4H), 7.29 (d, *J* = 4 Hz, 2H), 7.16-7.12 (m, 2H), 7.04 (s, 1H), 6.92 (m, 2H), 6.60 (d, *J* = 8 Hz, 2H), 5.76 (s, 1H), 4.11 (s, 2H); <sup>13</sup>C NMR (100 MHz, DMSO-*d*<sub>6</sub>) δ 159.67, 158.65, 157.53, 156.87, 149.37, 140.13, 137.40, 137.27, 129.81, 129.51, 129.25, 128.17, 123.08, 120.35, 19.28, 117.59, 113.42, 110.34, 109.94, 109.02, 106.77, 27.74. HRMS (ESI) *m/z* calculated for [M+H]<sup>+</sup>: 394.1668; found: 394.1656.

4.1.2. N-(3-((5,10-dihydropyrimido[4,5-b]quinolin-4-yl)amino)phenyl)-3-fluorobenamide (**12b**). Yellow solid; yield, 86.7%; mp, 232.7-233.2 °C; <sup>1</sup>H NMR (400 MHz, DMSO- *d*<sub>6</sub>) δ 10.18 (s, 1H), 9.94 (s, 1H), 8.25 (s, 1H), 7.92 (d, *J* = 8 Hz, 2H), 7.57-7.49 (m, 2H), 7.16-7.11 (m, 3H), 6.96-6.92 (m, 3H), 6.91 (d, *J* = 8 Hz, 1H), 5.07(s, 1H), 4.11 (s, 2H); <sup>13</sup>C NMR (100 MHz, DMSO- *d*<sub>6</sub>) δ 164.67, 158.86, 157.53, 156.69, 149.47, 139.92, 137.79, 133.65, 131.65, 130.82, 129.51, 129.33, 128.12, 127.88, 126.93, 123.08, 119.28, 115.89, 110.53, 109.94, 108.94, 106.71, 27.48. HRMS (ESI) *m/z* calculated for [M+H]<sup>+</sup>: 412.1574; found: 412.1560.

4.1.3. 3-chloro-N-(3-((5,10-dihydropyrimido[4,5-b]quinolin-4-yl)amino)phenyl)benzamide (**12c**). Yellow solid; yield, 87.3%; mp, 239.1-240.5 °C; <sup>1</sup>H NMR (400 MHz, DMSO-*d*<sub>6</sub>) δ 10.20 (s, 1H), 10.06 (s, 1H), 8.26 (s, 1H), 7.96 (s, 1H), 7.88 (d, *J* = 8 Hz, 1H), 7.65 (d, *J* = 8 Hz, 1H), 7.55 (dd, *J*<sub>1</sub> = *J*<sub>2</sub> = 8 Hz, 1H), 7.16-7.12 (m, 4H), 6.94-6.92 (m, 4H), 5.12 (s, 1H), 4.12 (s, 2H); <sup>13</sup>C NMR (100 MHz, DMSO- *d*<sub>6</sub>) δ 164.28, 158.67, 157.53, 156.86, 149.48, 139.79, 137.40, 134.15, 132.65, 130.82, 129.51, 128.12, 127.82, 126.93, 123.08, 119.28, 115.81, 110.53, 109.94, 108.94, 106.69, 27.74. HRMS (ESI) *m/z* calculated for [M+H]<sup>+</sup>: 428.1278; found: 428.1257.

4.1.4. N-(3-((5,10-dihydropyrimido[4,5-b]quinolin-4-yl)amino)phenyl)-3-methylbenz

-amide(**12d**). Yellow solid; yield, 83.1%; mp, 212.6-213.2 °C; <sup>1</sup>H NMR (400 MHz, DMSO-*d*<sub>6</sub>) δ 10.218 (s, 1H), 10.01 (s, 1H), 8.25 (s, 1H), 7.79-7.73 (m, 3H), 7.57 (s, *J* = 8 Hz, 1H), 7.42 (d, *J* = 8 Hz, 1H), 7.14-7.09 (m, 3H), 6.97-6.87 (m, 2H), 6.34 (m, 2H), 5.10 (s, 1H), 4.11 (s, 2H); <sup>13</sup>C NMR (100 MHz, DMSO- *d*<sub>6</sub>) δ 164.28, 158.67, 157.53, 156.86, 149.48, 139.97, 139.71, 137.42, 133.65, 131.65, 130.85, 129.56, 128.28, 127.88, 126.93, 123.18, 119.43, 115.81, 110.69, 109.94, 108.94, 106.56, 27.74, 19.07. HRMS (ESI) *m/z* calculated for [M+H]<sup>+</sup>: 408.1824; found: 408.1813.

4.1.5. N-(3-((5,10-dihydropyrimido[4,5-*b*]quinolin-4-yl)amino)phenyl)3-methoxybenzamide(**12e**). Yellow solid; yield, 80.3%; mp, 216.2-216.9 °C; <sup>1</sup>H NMR (400 MHz, DMSO-*d*<sub>6</sub>) δ 10.21 (s, 1H), 9.93 (s, 1H), 8.26 (s, 1H), 7.50 (d, *J* = 8 Hz, 1H), 7.44-7.40 (m, 2H), 7.16-7.10 (m, 3H), 7.08 (s, 1H), 6.98-6.90 (m, 3H), 6.85 (d, *J* = 8 Hz, 1H), 6.31 (d, *J* = 8 Hz, 1H), 5.11 (s, 1H), 4.11 (s, 2H), 3.83 (s, 3H); <sup>13</sup>C NMR (100 MHz, DMSO-*d*<sub>6</sub>) δ 159.65, 158.67, 157.53, 156.87, 149.42, 140.17, 137.40, 137.25, 129.96, 129.51, 129.27, 128.13, 123.08, 120.35, 119.28, 117.59, 115.81, 113.37, 110.34, 109.94, 109.02, 106.77, 55.84, 27.74. HRMS (ESI) *m/z* calculated for [M+H]<sup>+</sup>: 424.1773; found: 424.1760.

4.1.6. N-(3-((5,10-dihydropyrimido[4,5-*b*]quinolin-4-yl)amino)phenyl)-3-(trifluoromethyl)benzamide(**12f**). Yellow solid; yield, 78.3%; mp, 242.8-243.6 °C; <sup>1</sup>H NMR (400 MHz, DMSO-*d*<sub>6</sub>) δ 10.21 (s, 1H), 10.17 (s, 1H), 8.21 (s, 1H), 7.65 (m, 3H), 7.60 (d, *J* = 8 Hz, 1H), 7.54 (d, *J* = 8 Hz, 1H), 7.50 (d, *J* = 8 Hz, 1H), 7.43-7.41 (m, 2H), 7.33-7.31 (m, 2H), 7.15 (d, *J* = 8 Hz, 2H), 4.11 (s, 2H); <sup>13</sup>C NMR (100 MHz, DMSO-*d*<sub>6</sub>) δ 164.64, 164.59, 158.61, 157.50, 156.79, 150.55, 147.47, 137.87, 136.10, 132.30, 130.25, 129.43, 128.07, 125.32, 124.81, 123.06, 122.35, 122.06, 121.24, 119.20, 115.79, 109.82, 27.72. HRMS (ESI) *m/z* calculated for [M+H]<sup>+</sup>: 462.1542; found: 462.1520.

4.1.7. N-(4-((5,10-dihydropyrimido[4,5-*b*]quinolin-4-yl)amino)phenyl)benzamide (**13a**). Yellow solid; yield, 88.3%; mp, 201.4-202.6 °C; <sup>1</sup>H NMR (400 MHz,

DMSO- $d_6$ )  $\delta$  10.21 (s, 1H), 9.96 (s, 1H), 8.26 (s, 1H), 7.78 (dd,  $J_1 = 8$  Hz,  $J_2 = 4$  Hz, 2H), 7.56-7.47 (d,  $J = 8$  Hz, 1H), 7.41-7.35 (m, 3H), 7.16-7.12 (m, 2H), 6.93-6.92 (m, 2H), 6.54 (d,  $J = 8$  Hz, 2H), 6.37 (s, 1H) 5.01 (s, 1H), 4.11 (s, 2H);  $^{13}\text{C}$  NMR (100 MHz, DMSO- $d_6$ )  $\delta$  158.67, 158.42, 157.15, 149.13, 141.53, 140.89, 140.16, 1400.00, 136.43, 135.45, 134.65, 129.25, 127.29, 125.60, 122.89, 122.36, 18.99, 118.60, 12.95, 110.99, 106.05, 27.62. HRMS (ESI)  $m/z$  calculated for  $[\text{M}+\text{H}]^+$ : 394.1668; found: 394.1650.

4.1.8. N-(4-((5,10-dihydropyrimido[4,5-b]quinolin-4-yl)amino)phenyl)-3-fluorobenzamide(**13b**). Yellow solid; yield, 89.1%; mp, 213.3-214.4 °C;  $^1\text{H}$  NMR (400 MHz, DMSO- $d_6$ )  $\delta$  10.21 (s, 1H), 9.96 (s, 1H), 8.26(s, 1H), 7.79-7.77 (m, 2H), 7.74 (d,  $J = 8.0$ Hz, 1H), 7.60-7.54 (m, 1H), 7.41-7.35 (m, 3H), 7.16-7.12 (m, 2H), 6.92 (d,  $J = 8$  Hz, 2H), 6.52 (d,  $J = 8$  Hz, 1H), 5.01 (s, 1H), 4.12(s, 2H);  $^{13}\text{C}$  NMR (100 MHz, DMSO- $d_6$ )  $\delta$  158.42, 157.15, 156.86, 150.13, 141.53, 140.89, 140.16, 140.03, 136.45, 135.44, 134.63, 129.29, 127.25, 125.60, 122.86, 122.33, 118.99, 118.62, 112.95, 110.99, 106.00, 27.65. HRMS (ESI)  $m/z$  calculated for  $[\text{M}+\text{H}]^+$ : 412.1574; found: 412.1549.

4.1.9. 3-chloro-N-(4-((5,10-dihydropyrimido[4,5-b]quinolin-4-yl)amino)phenyl)-benzamide(**13c**). Yellow solid; yield, 90.6%; mp, 220.1-221.3 °C;  $^1\text{H}$  NMR (400 MHz, DMSO- $d_6$ )  $\delta$  10.21 (s, 1H), 9.96 (s, 1H), 8.26 (s, 1H), 7.78 (d,  $J = 8$  Hz, 1H), 7.76 (d,  $J = 8$  Hz, 1H), 7.56 (d,  $J = 8$  Hz, 1H), 7.39 (d,  $J = 8$  Hz, 1H), 7.38-7.35 (m, 2H), 7.16-7.12(m, 2H), 6.92 (d,  $J = 8$  Hz, 2H), 6.54 (d,  $J = 8$  Hz, 2H), 5.01 (s, 1H), 4.12 (s, 2H);  $^{13}\text{C}$  NMR (100 MHz, DMSO- $d_6$ )  $\delta$  163.61, 158.67, 155.53, 156.86, 145.94, 137.83, 137.40, 133.66, 131.43, 130.79, 129.50, 128.32, 128.12, 127.71, 126.74, 123.07, 122.75, 119.27, 115.81, 114.18, 109.93, 27.74. HRMS (ESI)  $m/z$  calculated for  $[\text{M}+\text{H}]^+$ : 428.1278; found: 428.1256.

4.1.10. N-(4-((5,10-dihydropyrimido[4,5-b]quinolin-4-yl)amino)phenyl)-3-methylbenzamide(**13d**). Yellow solid; yield, 80.5%; mp, 214.8-215.6 °C;  $^1\text{H}$  NMR (400 MHz,

DMSO- $d_6$ )  $\delta$  10.21 (s, 1H), 9.90 (s, 1H), 8.26 (s, 1H), 7.92 (d,  $J = 8$  Hz, 2H), 7.53-7.48 (m, 2H), 7.38(d,  $J = 8$  Hz, 2H), 7.16-7.10 (m, 2H), 6.93-6.90 (m, 2H), 6.55 (d,  $J = 8$  Hz, 2H), 5.23 (s, 1H), 4.09 (s, 2H), 2.09 (s, 3H);  $^{13}\text{C}$  NMR (100 MHz, DMSO- $d_6$ )  $\delta$  164.61, 158.54, 157.51, 156.79, 139.07, 138.06, 137.35, 136.85, 136.09, 134.39, 132.31, 129.42, 128.22, 125.25, 123.06, 122.30, 122.06, 121.24, 119.20, 115.82, 109.87, 27.72, 19.04. HRMS (ESI)  $m/z$  calculated for  $[\text{M}+\text{H}]^+$ : 408.1824; found: 408.1809.

4.1.11. N-(4-((5,10-dihydropyrimido[4,5-b]quinolin-4-yl)amino)phenyl)-3-methoxy-benzamide(**13e**). Yellow solid; yield, 78.6%; mp, 228.8-229.6 °C;  $^1\text{H}$  NMR (400 MHz, DMSO- $d_6$ )  $\delta$  10.21 (s, 1H), 9.87 (s, 1H), 8.27 (s, 1H), 7.51 (d,  $J = 8$  Hz, 1H), 7.46 (s,  $J = 8$  Hz, 1H), 7.42 (d,  $J = 8$  Hz, 1H), 7.37 (d,  $J = 8$  Hz, 2H), 7.17-7.11 (m, 3H), 6.94 (d,  $J = 8$  Hz, 2H), 6.55 (d,  $J = 8$  Hz, 2H), 4.13 (s, 2H), 3.84 (s, 3H);  $^{13}\text{C}$  NMR (100 MHz, DMSO- $d_6$ )  $\delta$  158.67, 157.53, 156.86, 153.13, 141.53, 140.89, 136.45, 135.44, 134.63, 128.27, 126.29, 125.20, 122.69, 121.86, 118.29, 117.90, 112.95, 110.96, 106.95, 104.03, 56.62, 27.52. HRMS (ESI)  $m/z$  calculated for  $[\text{M}+\text{H}]^+$ : 424.1773; found: 424.1765.

4.1.12. N-(4-((5,10-dihydropyrimido[4,5-b]quinolin-4-yl)amino)phenyl)-3-(trifluoromethyl)benzamide(**13f**). Yellow solid; yield, 70.5%; mp, 240.6-241.9 °C;  $^1\text{H}$  NMR (400 MHz, DMSO- $d_6$ )  $\delta$  10.18 (s, 1H), 9.94 (s, 1H), 8.25 (s, 1H), 7.92 (d,  $J = 8$  Hz, 2H), 7.57-7.49 (m, 2H), 7.16-7.11 (m, 3H), 6.96-6.92 (m, 3H), 6.31 (d,  $J = 8$  Hz, 2H), 5.07 (s, 1H), 4.11 (s, 2H);  $^{13}\text{C}$  NMR (100 MHz, DMSO- $d_6$ )  $\delta$  164.79, 164.49, 158.54, 157.51, 156.82, 142.13, 139.07, 138.06, 137.35, 136.85, 136.09, 134.39, 129.42, 128.22, 125.25, 123.06, 122.30, 122.06, 121.24, 119.20, 115.87, 109.82, 27.72. HRMS (ESI)  $m/z$  calculated for  $[\text{M}+\text{H}]^+$ : 462.1542; found: 462.1528.

4.1.13. 1-(4-((5,10-dihydropyrimido[4,5-b]quinolin-4-yl)amino)phenyl)-3-phenylurea (**14a**). Yellow solid; yield, 67.5%; mp, 251.6-252.8 °C;  $^1\text{H}$  NMR (400 MHz, DMSO- $d_6$ )  $\delta$  10.58 (s, 1H), 10.27 (s, 1H), 9.34 (s, 1H), 8.20 (s, 1H), 7.55-7.51 (m,

3H), 7.48-7.39 (m, 3H), 7.26-7.21 (m, 3H), 7.19-7.11 (m, 2H), 7.07-7.01 (m, 2H), 4.10 (s, 2H);  $^{13}\text{C}$  NMR (100 MHz, DMSO- $d_6$ )  $\delta$  158.35, 157.12, 156.13, 149.23, 140.17, 139.37, 136.00, 134.32, 129.26, 128.68, 128.27, 126.14, 122.35, 121.38, 119.32, 118.58, 115.27, 111.83, 108.03, 28.00. HRMS (ESI)  $m/z$  calculated for  $[\text{M}+\text{H}]^+$ : 409.1777; found 409.1753.

4.1.14. 1-(4-((5,10-dihydropyrimido[4,5-b]quinolin-4-yl)amino)phenyl)-3-(3-fluorophenyl)urea(**14b**). Yellow solid; yield, 77.5%; mp, 261.6-262.7 °C;  $^1\text{H}$  NMR (400 MHz, DMSO- $d_6$ )  $\delta$  10.58 (s, 1H), 10.27 (s, 1H), 9.49 (s, 1H), 8.68 (s, 1H), 8.40 (s, 1H), 7.60 (d,  $J = 8$  Hz, 2H), 7.51 (d,  $J = 8$  Hz, 1H), 7.39 (d,  $J = 8$  Hz, 1H), 7.34-7.28 (m, 3H), 7.12(d,  $J = 8$  Hz, 1H), 7.06 (d,  $J = 8$  Hz, 2H), 7.01 (d,  $J = 8$  Hz, 2H), 4.11 (s, 2H);  $^{13}\text{C}$  NMR (100 MHz, DMSO- $d_6$ )  $\delta$  161.71, 158.67, 157.53, 156.86, 152.95, 150.21, 141.99, 141.61, 140.39, 139.06, 130.75, 128.94, 126.61, 124.54, 124.33, 119.72, 116.23, 115.02, 114.31, 108.73, 108.52, 105.35, 105.08, 27.61. HRMS (ESI)  $m/z$  calculated for  $[\text{M}+\text{H}]^+$ : 427.1683; found: 427.1661.

4.1.15. 1-(3-chlorophenyl)-3-(4-((5,10-dihydropyrimido[4,5-b]quinolin-4-yl)amino)phenyl)urea(**14c**). Yellow solid; yield, 87.6%; mp, 269.8-270.6 °C;  $^1\text{H}$  NMR (400 MHz, DMSO- $d_6$ )  $\delta$  10.27 (s, 1H), 9.88 (s, 1H), 9.52 (s, 1H), 8.67 (s, 1H), 8.39 (s, 1H), 7.69 (s, 1H), 7.65 (d,  $J = 8$  Hz, 1H), 7.60 (d,  $J = 8$  Hz, 2H), 7.38 (s, 1H), 7.31-7.28 (m, 4H), 7.00 (d,  $J = 8$  Hz, 2H), 6.97-6.94 (m, 2H), 6.92-6.84 (m, 2H), 4.11 (s, 2H);  $^{13}\text{C}$  NMR (100 MHz, DMSO- $d_6$ )  $\delta$  158.80, 156.99, 155.59, 150.50, 141.00, 140.16, 136.44, 130.25, 128.97, 126.05, 125.67, 124.86, 123.35, 122.16, 119.73, 118.64, 116.62, 115.20, 114.47, 27.43. HRMS (ESI)  $m/z$  calculated for  $[\text{M}+\text{H}]^+$ : 423.1387; found: 423.1367.

4.1.16. 1-(4-((5,10-dihydropyrimido[4,5-b]quinolin-4-yl)amino)phenyl)-3-(*m*-tolyl)urea(**14d**). Yellow solid; yield, 75.5%; mp, 255.2-256.4 °C;  $^1\text{H}$  NMR (400 MHz, DMSO- $d_6$ )  $\delta$  9.32 (s, 1H), 9.14 (s, 1H), 8.71 (s, 1H), 8.22 (s, 1H), 7.65-7.56 (m, 3H), 7.47 (d,  $J = 8$  Hz, 2H), 7.29 (d,  $J = 8$  Hz, 1H), 7.26-7.23 (m, 2H), 7.06 (d,  $J = 8$  Hz,

2H), 7.02 (d,  $J = 8$  Hz, 2H), 4.21 (s, 2H), 2.02 (s, 3H);  $^{13}\text{C}$  NMR (100 MHz, DMSO- $d_6$ )  $\delta$  158.35, 157.12, 155.20, 152.95, 150.10, 141.74, 141.58, 140.35, 135.75, 133.70, 130.87, 128.93, 126.60, 124.60, 124.36, 121.92, 119.71, 117.87, 116.94, 116.23, 115.03, 27.28, 20.58. HRMS (ESI)  $m/z$  calculated for  $[\text{M}+\text{H}]^+$ : 423.1933; found: 423.1899.

4.1.17. 1-(4-((5,10-dihydropyrimido[4,5-b]quinolin-4-yl)amino)phenyl)-3-(3-methoxyphenyl)urea (**14e**). Yellow solid; yield, 76.5%; mp, 265.7-266.7 °C;  $^1\text{H}$  NMR (400 MHz, DMSO- $d_6$ )  $\delta$  9.32 (s, 1H), 9.14 (s, 1H), 8.71 (s, 1H), 8.23 (s, 1H), 7.64 (d,  $J = 8$  Hz, 1H), 7.62-7.56 (m, 2H), 7.45 (dd,  $J_1 = 8$  Hz,  $J_2 = 4$  Hz 2H), 7.29 (d,  $J = 8$  Hz, 1H), 7.25 (dd,  $J_1 = 8$  Hz,  $J_2 = 4$  Hz 2H), 7.16-7.12 (m, 2H), 6.93-6.91 (m, 2H), 4.14 (s, 2H), 3.73 (s, 3H);  $^{13}\text{C}$  NMR (100 MHz, DMSO- $d_6$ )  $\delta$  158.35, 157.12, 155.86, 153.12, 140.15, 139.64, 134.75, 128.38, 126.65, 125.99, 125.90, 124.05, 122.77, 122.34, 121.79, 120.47, 119.89, 115.14, 113.79, 106.95, 56.19, 27.25. HRMS (ESI)  $m/z$  calculated for  $[\text{M}+\text{H}]^+$ : 439.1882; found: 439.1875.

4.1.18. 1-(4-((5,10-dihydropyrimido[4,5-b]quinolin-4-yl)amino)phenyl)-3-(3(trifluoromethyl)phenyl)urea (**14f**). Yellow solid; yield, 70.5%; mp, 275.4-276.8 °C;  $^1\text{H}$  NMR (400 MHz, DMSO- $d_6$ )  $\delta$  10.21 (s, 1H), 9.74 (s, 1H), 9.67 (s, 1H), 8.81 (s, 1H), 8.47 (s, 1H), 7.65 (d,  $J = 8$  Hz, 2H), 7.60 (d,  $J = 8$  Hz, 1H), 7.53 (d,  $J = 8$  Hz, 1H), 7.50 (d,  $J = 8$  Hz, 1H), 7.42 (d,  $J = 8$  Hz, 2H), 7.32 (d,  $J = 8$  Hz, 2H), 7.16-7.14 (m, 2H), 6.93-6.91 (m, 2H), 4.18 (s, 2H);  $^{13}\text{C}$  NMR (100 MHz, DMSO- $d_6$ )  $\delta$  164.23, 158.42, 157.15, 156.13, 148.23, 141.53, 140.89, 136.45, 135.44, 134.63, 129.27, 127.29, 125.60, 122.89, 122.36, 118.99, 118.60, 112.95, 112.03, 106.65, 27.62. HRMS (ESI)  $m/z$  calculated for  $[\text{M}+\text{H}]^+$ : 476.1572; found: 476.1552.

#### 4.2. Molecular docking

The molecular modeling of compound **13b** was performed with Discovery Studio.3.1/CDOCKER protocol (Accelrys Software Inc.). The dimensional structure of EGFR (PDB ID: 1M17) and Src (PDB ID: 3G6H) was downloaded from Protein

Data Bank (PDB). The following process was used to carry out molecular docking: (1) deleting the water crystallization involved in protein kinase structure; (2) optimizing protein structure and ligands; (3) defining receptor and ligand, finding the candidate binding site; (4) deleting small molecular docking in candidate binding site; (5) docking designed compounds into the candidate binding site on the target protein kinase; (6) molecular modeling based on the above docking data.

#### 4.3. Cell Antiproliferation Assay

Cell antiproliferation assay based on MTT were performed with 2 cancer cell lines. Briefly, 100  $\mu\text{L}$  of K562 cell solution with the concentration of  $7 \times 10^5$  cells  $\text{mL}^{-1}$  was seeded to each well of a 96-well plate and incubated for 12 h at 37 °C in a 5%  $\text{CO}_2$  incubator. The test compound solution was added to each well for the treatment of maintained cells in triplicate per concentration, and incubated at 37 °C in a 5%  $\text{CO}_2$  incubator for 48 h. After this treatment, 10  $\mu\text{L}$  MTT solution ( $5 \text{ mg mL}^{-1}$ ) was then added to each well and incubated for 4 h at 37 °C. The formazan precipitate was dissolved in 100  $\mu\text{L}$  DMSO and the absorbance at 490 nm was determined using Multimode Detector DTX880 (Beckman Coulter).

A549 cells were seeded in 96-well plates at a density of  $5-7 \times 10^3$  cells per well with incubation overnight in a 5%  $\text{CO}_2$  incubator at 37 °C, the growth medium in each well was then exchanged with 0.1 mL of fresh medium containing graded concentrations of compounds to be tested or equal DMSO and incubated continuously for 48 h. Then 10  $\mu\text{L}$  MTT solution ( $5 \text{ mg mL}^{-1}$ ) was added to each well, and the cells were incubated for additional 4 h. The MTT - formazan crystals were dissolved in 100  $\mu\text{L}$  of DMSO, the absorbance of each well was measured at 490 nm using an automatic ELISA reader system (TECAN, CHE). Etoposide and Doxorubicin was used as positive controls.

#### 4.4. Kinase Inhibition Assays

*In vitro* kinase assays were carried out by Medicilon Co., Ltd in Shanghai, China. Kinases inhibitory activities of synthetic compounds against EGFR and Src. The

general procedures were as follows: mix enzyme, substrate, ATP and compounds in a buffer solution (pH = 7.0) of 50 mM HEPES/NaOH, 0.02% NaN<sub>3</sub>, 0.01% BSA, 0.1 mM Mortho-vanadate, 5 mM MgCl<sub>2</sub>, 1 mM DTT in an OptiPlate-384. The assay plate was incubated at room temperature for 15 min and compounds in 10 μM dissolved in 2.5% DMSO. Then the mixture were added by Streptavidin-XL665 and TK antibody europium cryptate (1:100) solution 10 μL (50 mM HEPES/NaOH pH = 7.0, 0.1% BSA, 0.8 M KF, 20 mM EDTA). The Instrument (Perkinelmer) to detect the signal at room temperature. The luminescence was read at envision. The signal was correlated with the amount of ATP remaining in the reaction and was inversely correlated with the kinase activity.

#### 4.5. Western Blot Analysis

K562 cells were treated with vehicle or different concentration of **13b** for 48 h, whole cell proteins were extracted by RIPA lysis as described. The concentrations of the cell lysates were measured by the DC Protein Assay Kit I from Bio-Rad (California, USA). Equal amounts of protein were subjected to 10% SDS polyacrylamide gel electrophoresis followed by transferring to PVDF membranes, and were subsequently analyzed with EGFR, p-EGFR, Src and p-Src antibodies from Cell Signalling (MA, USA). Specific protein signals from their respective horseradish peroxidase linked secondary antibodies were detected and measured by the Luminescence Image Analyzer Tanon 5200 (Shanghai, China). The density of the bands were measured by Image Quant software (Molecular Dynamics, Sunnyvale, CA, USA), and then expressed as the percentage of the density of the β-actin band.

#### 4.6. Cell invasion assay

Cell invasion assay was performed as described [51]. Invasion inserts with 8 μm pore membranes from Corning (New York, USA) were coated with fibronectin from Sigma-Aldrich (Missouri, USA) as described [52]. A549 cells were pretreated with different concentration of **13b** for 6 h, respectively. The pretreated cells were seeded on the inserts to reach confluence in 12 h, and then culture for another 24 h with drug

treatment. After fixed with 4% formaldehyde, non-invading cells on the upper side of the membranes were removed by cotton swab. The invading cells were stained with 0.08% trypan blue for 15 min as described [53] and were photographed by a bright-field light microscope. Cell numbers of five random views were counted by Image-Pro-Plus 6.0 of Media Cybernetics (MD, USA).

#### 4.7. Cell Apoptosis Assays

A total of  $1 \times 10^5$  cells mL<sup>-1</sup> K562 cells were plated in a six-well plate and treated with **13b** for 48 h at 37 °C. After incubation, the cells were harvested and washed with ice-cold PBS. The cell cycle progression was analyzed using an apoptosis analysis kit (Beyotime), and the apoptosis ratio was performed with an annexin V-FITC Apoptosis Detection Kit (keygentec).

#### Acknowledgments

The authors would like to thank the financial supports from Shenzhen Municipal Development and Reform Commission (Disciplinary Development Program for Chemical Biology), the financial supports from the Chinese National Natural Science Foundation (21372141), and Shenzhen Sci & Tech Bureau (CXB201104210013A, CXZZ20150529165045064 and JCYJ20150331151358131).

#### Conflict of Interest

The authors declare no conflicts of interest.

#### Appendix A. Supplementary material

Supplementary data (<sup>1</sup>H NMR, <sup>13</sup>C NMR and 2D spectra of compound **4** and **5**; the UV-vis absorption spectra of compound **13b** binding with ct DNA, <sup>1</sup>H NMR and <sup>13</sup>C NMR spectra and high resolution mass spectrometry of **12-14 (a-f)**) associated with this article can be found in the online version.

#### References

- [1] L.Z. Zhang, Y.M. Li, L. Lan, R. Liu, Y.H. Wu, Q.X. Qu, K. Wen, Tamoxifen Has a Proliferative Effect in Endometrial Carcinoma Mediated via The GPER/EGFR/ERK/cyclin D1 Pathway: A Retrospective Study and an *in vitro* Study, *Mol. Cell Endocrinol.*, 437 (2016) 51-61.
- [2] Y.J. Chen, K.N. Lin, L.M. Jhang, C.H. Huang, Y.C. Lee, L.S. Chang, Gallic Acid Abolishes the EGFR/Src/Akt/Erk-mediated Expression of Matrix Metalloproteinase-9 in MCF-7 Breast Cancer Cells, *Chem. Biol. Interact.*, 252 (2016) 131-140.
- [3] S.V. Sharma, D.W. Bell, J. Settleman, D.A. Haber, Epidermal Growth Factor Receptor Mutations in Lung Cancer, *Nat. Rev. Cancer*, 7 (2007) 169-181.
- [4] L.A. Bazley, W.J. Gullick, The Epidermal Growth Factor Receptor Family, *Endocr. Relat. Cancer*, 12 (2005) S17-S27.
- [5] C.D. Andl, T. Mizushima, K. Oyama, M. Bowser, H. Nakagawa, A.K. Rustgi, EGFR-induced Cell Migration is Mediated Predominantly by The JAK-STAT Pathway in Primary Esophageal Keratinocytes, *Am. J. Physiol. Gastrointestinal and Liver Physiology*, 287 (2004) G1227-G1237.
- [6] M.J. Lavecchia, R. Puig de la Bellacasa, J.I. Borrell, C.N. Cavasotto, Investigating Molecular Dynamics-guided Lead Optimization of EGFR Inhibitors, *Bioor. Med. Chem.*, 24 (2016) 768-778.
- [7] S. Rao, A.L. Larroque-Lombard, L. Peyrard, C. Thauvin, Z. Rachid, C. Williams, B.J. Jean-Claude, Target Modulation by a Kinase Inhibitor Engineered to Induce a Tandem Blockade of The Epidermal Growth Factor Receptor (EGFR) and c-Src: The Concept of Type III Combi-targeting, *PLoS One*, 10 (2015) e0117215.
- [8] F.R. Hirsch, M. Varella-Garcia, P.A. Bunn, M.V. Di Maria, R. Veve, R.M. Bremnes, A.E. Baron, C. Zeng, W.A. Franklin, Epidermal Growth Factor Receptor in Non-small-cell lung Carcinomas: Correlation Between Gene Copy Number and Protein Expression and Impact on Prognosis, *J. Clin. Oncol.*, 21 (2003) 3798-3807.
- [9] H.Q. Zhang, F.H. Gong, C.G. Li, C. Zhang, Y.J. Wang, Y.G. Xu, L.P. Sun, Design and Discovery of 4-anilinoquinazoline-acylamino Derivatives as EGFR and

- VEGFR-2 Dual TK Inhibitors, *Eur. J. Med. Chem.*, 109 (2016) 371-379.
- [10] E. Sundby, J. Han, S.J. Kaspersen, B.H. Hoff, *In vitro* Baseline of New Pyrrolopyrimidine EGFR-TK Inhibitors with Erlotinib, *Eur. J. Pharm. Sci.*, 80 (2015) 56-65.
- [11] F. Tan, Y. Shi, Y. Wang, L. Ding, X. Yuan, Y. Sun, Icotinib, a Selective EGF Receptor Tyrosine Kinase Inhibitor, for the Treatment of Non-small-cell Lung Cancer, *Future Oncol.*, 11 (2015) 385-397.
- [12] K. Bouchalova, M. Cizkova, K. Cwiertka, R. Trojanec, D. Friedecky, M. Hajduch, Lapatinib in Breast Cancer -the Predictive Significance of Her1 (EGFR), Her2, Pten and PIK3CA Genes and Lapatinib Plasma Level Assessment, *Biom. Pap. Olomouc*, 154 (2010) 281-288.
- [13] L. Tao, F. Zhu, F. Xu, Z. Chen, Y.Y. Jiang, Y.Z. Chen, Co-targeting Cancer Drug Escape Pathways Confers Clinical Advantage for Multi-target Anticancer Drugs, *Pharm. Res.*, 102 (2015) 123-131.
- [14] C.E. Steuer, S.S. Ramalingam, Targeting EGFR in Lung Cancer: Lessons Learned and Future Perspectives, *Mol. Aspects Med.*, 45 (2015) 67-73.
- [15] Q. Chen, Z. Zhou, L. Shan, H. Zeng, Y. Hua, Z. Cai, The Importance of Src Signaling in Sarcoma, *Oncol. Lett.*, 10 (2015) 17-22.
- [16] G.H. Zeng, D.Q. Fang, W.J. Wu, J.P. Wang, W.G. Xie, S.J. Ma, J.H. Wu, Y. Shen, Theoretical Studies on Pyrazolo 3,4-d pyrimidine Derivatives as Potent Dual c-Src/Abl Inhibitors Using 3D-QSAR and Docking Approaches, *Mol. Inform.*, 33 (2014) 183-200.
- [17] M.M.M. Copiz, T.A.S. Coloma, c- Src and Its Role in Cystic Fibrosis, *Eur. J. Cell Biol.*, 95 (2016) 401-413.
- [18] C.H. Zhang, M.W. Zheng, Y.P. Li, X.D. Lin, M. Huang, L. Zhong, G.B. Li, R.J. Zhang, W.T. Lin, Y. Jiao, X.A. Wu, J. Yang, R. Xiang, L.J. Chen, Y.L. Zhao, W. Cheng, Y.Q. Wei, S.Y. Yang, Design, Synthesis, and Structure-Activity Relationship Studies of 3-(Phenylethynyl)-1H-pyrazolo[3,4-d]pyrimidin-4-amine Derivatives as a New Class of Src Inhibitors with Potent Activities in Models of Triple Negative Breast Cancer, *J. Med. Chem.*, 58 (2015) 3957-3974.

- [19] R. Roskoski, Src Protein-tyrosine Kinase Structure, Mechanism, and Small Molecule Inhibitors, *Pharm. Res.*, 94 (2015) 9-25.
- [20] A. Kumar, A.S. Jaggi, N. Singh, Pharmacology of Src Family Kinases and Therapeutic Implications of Their Modulators, *Fundam. Clin. Pharmacol.*, 29 (2015) 115-130.
- [21] E.M.H. Kim, K. Mueller, E. Gartner, J. Boerner, Dasatinib is Synergistic with Cetuximab and Cisplatin in Triple-negative Breast Cancer Cells, *J. Surg. Res.*, 185 (2013) 231-239.
- [22] E. Giovannetti, M. Labots, H. Dekker, E. Galvani, J.S.W. Lind, R. Sciarrillo, R. Honeywell, E.F. Smit, H.M. Verheul, G.J. Peters, Molecular Mechanisms and Modulation of Key Pathways Underlying the Synergistic Interaction of Sorafenib with Erlotinib in Non-Small-Cell-Lung Cancer (NSCLC) Cells, *Curr. Pharm. Design*, 19 (2013) 927-939.
- [23] L. Formisano, L. Nappi, R. Rosa, R. Marciano, C. D'Amato, V. D'Amato, V. Damiano, L. Raimondo, F. Iommelli, A. Scorziello, G. Troncone, B.M. Veneziani, S.J. Parsons, S. De Placido, R. Bianco, Epidermal Growth Factor-Receptor Activation Modulates Src-dependent Resistance to Lapatinib in Breast Cancer Models, *Breast Cancer Res.*, 16 (2014).
- [24] Y.L. Pan, M.W. Zheng, L. Zhong, J. Yang, S. Zhou, Y. Qin, R. Xiang, Y.Z. Chen, S.Y. Yang, A Preclinical Evaluation of SKLB261, a Multikinase Inhibitor of EGFR/Src/VEGFR2, as a Therapeutic Agent against Pancreatic Cancer, *Mol. Cancer Ther.*, 14 (2015) 407-418.
- [25] J.R. Tonra, M. Poyurovsky, K.G. Liu, J. Patel, N. Rao, R. Tilton, J.L. Ryan, M.S. Berger, L. Witte, J.I. Kim, S.D. Waksal, KD019: Blood Brain Barrier Penetrant HER2/neu, Src, and EGFR Inhibitor, *Cancer Res.*, 75 (2015).
- [26] W. Zhang, B. Zhang, W. Zhang, T. Yang, N. Wang, C.M. Gao, C.Y. Tan, H.X. Liu, Y.Y. Jiang, Synthesis and Antiproliferative Activity of 9-benzylamino-6-chloro-2-methoxy-acridine Derivatives as Potent DNA-binding Ligands and Topoisomerase II Inhibitors, *Eur. J. Med. Chem.*, 116 (2016) 59-70.
- [27] Y.N. Wang, D. Gao, B.Z. Chu, C.M. Gao, D.L. Cao, H.X. Liu, Y.Y. Jiang,

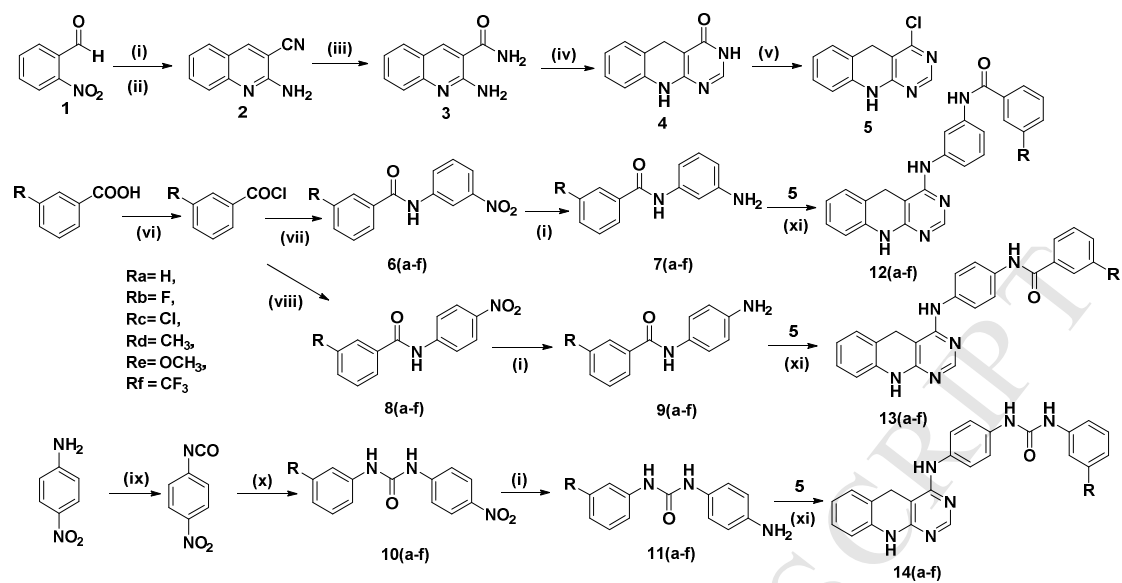
- Exposure of CCRF-CEM Cells to Acridone Derivative 8a Triggers Tumor Death via Multiple Mechanisms, *Proteomics*, 16 (2016) 1177-1190.
- [28] B. Zhang, K. Chen, N. Wang, C.M. Gao, Q.S. Sun, L.L. Li, Y.Z. Chen, C.Y. Tan, H.X. Liu, Y.Y. Jiang, Molecular Design, Synthesis and Biological Research of Novel Pyridyl Acridones as Potent DNA-binding and Apoptosis-inducing Agents, *Eur. J. Med. Chem.*, 93 (2015) 214-226.
- [29] J.P. Yu, H. Tian, C. Gao, H.J. Yang, Y.Y. Jiang, H. Fu, Boron-Catalyzed Arylthiooxygenation of N-Allylamides: Synthesis of (Arylsulfanyl)oxazolines, *Synlett*, 26 (2015) 676-680.
- [30] X. Li, C.M. Gao, T. Yang, B. Zhang, C.Y. Tan, H.X. Liu, Y.Y. Jiang, A POCl<sub>3</sub>-Mediated Synthesis of Substituted Fused Azoacridones Derivatives, *RSC Adv.*, 5 (2015) 28670-28678.
- [31] C.M. Gao, W. Zhang, S.N. He, S.F. Li, F. Liu, Y.Y. Jiang, Synthesis and Antiproliferative Activity of 2,7-diamino 10-(3,5-dimethoxy)benzyl-9(10H)-acridone Derivatives as Potent Telomeric G-quadruplex DNA Ligands, *Bioorg. Chem.*, 60 (2015) 30-36.
- [32] C.M. Gao, B. Li, B. Zhang, Q.S. Sun, L.L. Li, X. Li, C.J. Chen, C.Y. Tan, H.X. Liu, Y.Y. Jiang, Synthesis and Biological Evaluation of Benzimidazole Acridine Derivatives as Potential DNA-binding and Apoptosis-inducing Agents, *Bioorg. Med. Chem.*, 23 (2015) 1800-1807.
- [33] K. Chen, B.Z. Chu, F. Liu, B. Li, C.M. Gao, L.L. Li, Q.S. Sun, Z.F. Shen, Y.Y. Jiang, New Benzimidazole Acridine Derivative Induces Human Colon Cancer Cell Apoptosis *in vitro* via The ROS-JNK Signaling Pathway, *Acta. Pharm. Sin.*, 36 (2015) 1074-1084.
- [34] J.H. Jiang, C. Ding, L.L. Li, C.M. Gao, Y.Y. Jiang, C.Y. Tan, R.M. Hua, Synthesis and Antiproliferative Activity of RITA and Its Analogs, *Tetrahedron Lett.*, 55 (2014) 6635-6638.
- [35] Y.N. Wang, D. Gao, Z. Chen, S.F. Li, C.M. Gao, D.L. Cao, F. Liu, H.X. Liu, Y. Jiang, Acridone Derivative 8a Induces Oxidative Stress-Mediated Apoptosis in CCRF-CEM Leukemia Cells: Application of Metabolomics in Mechanistic

- Studies of Antitumor Agents, *Plos One*, 8 (2013).
- [36] X.L. Lang, L.L. Li, Y.Z. Chen, Q.S. Sun, Q. Wu, F. Liu, C.Y. Tan, H.X. Liu, C.M. Gao, Y.Y. Jiang, Novel Synthetic Acridine Derivatives as Potent DNA-binding and Apoptosis-inducing Antitumor Agents, *Bioorg. Med. Chem.*, 21 (2013) 4170-4177.
- [37] J.S. Lin, X.L. Jin, Y.W. Bu, D.L. Cao, N.N. Zhang, S.F. Li, Q.S. Sun, C.Y. Tan, C.M. Gao, Y.Y. Jiang, Efficient Synthesis of RITA and Its Analogues: Derivation of Analogues with Improved Antiproliferative Activity via Modulation of p53/miR-34a pathway, *Org. Biomol. Chem.*, 10 (2012) 9734-9746.
- [38] F. Jin, N.N. Zhang, C.Y. Tan, D. Gao, C.L. Zhang, F. Liu, Z. Chen, C.M. Gao, H.X. Liu, S.F. Li, Y.Y. Jiang, 2'-Chloro-4'-aminoflavone Derivatives Selectively Targeting Hepatocarcinoma Cells: Convenient Synthetic Process, G2/M Cell Cycle Arrest and Apoptosis Triggers, *Archiv. Der. Pharmazie*, 345 (2012) 525-534.
- [39] C.M. Gao, S.F. Li, X.L. Lang, H.X. Liu, F. Liu, C.Y. Tan, Y.Y. Jiang, Synthesis and Evaluation of 10-(3,5-dimethoxy)benzyl-9(10H)-acridone derivatives as selective telomeric G-quadruplex DNA ligands, *Tetrahedron*, 68 (2012) 7920-7925.
- [40] X.M. Hu, C.M. Gao, C.Y. Tan, C.L. Zhang, H.L. Zhang, S.F. Li, H.X. Liu, Y.Y. Jiang, Design and Synthesis of N-phosphoryl Peptide Modified Podophyllotoxin Derivatives as Potent Anticancer Agents, *Protein Peptide Lett.*, 18 (2011) 1258-1264.
- [41] H.C. Liu, A.J. Dong, C.M. Gao, C.Y. Tan, Z.H. Xie, X.Y. Zu, L. Qu, Y.Y. Jiang, New Synthetic Flavone Derivatives Induce Apoptosis of Hepatocarcinoma Cells, *Bioorg. Med. Chem.*, 18 (2010) 6322-6328.
- [42] C.M. Gao, F. Liu, X.D. Luan, C.Y. Tan, H.X. Liu, Y.H. Xie, Y.B. Jin, Y.Y. Jiang, Novel Synthetic 2-amino-10-(3,5-dimethoxy)benzyl-9(10H)-acridinone Derivatives as Potent DNA-binding Antiproliferative Agents, *Bioorg. Med. Chem.*, 18 (2010) 7507-7514.
- [43] Z. Cui, X. Li, L. Li, B. Zhang, C. Gao, Y. Chen, C. Tan, H. Liu, W. Xie, T. Yang, Y. Jiang, Design, Synthesis and Evaluation of Acridine Derivatives as Multi-target

- Src and MEK Kinase Inhibitors for Anti-tumor Treatment, *Bioorg. Med. Chem.*, 24 (2016) 261-269.
- [44] X.D. Luan, C.M. Gao, N.N. Zhang, Y.Z. Chen, Q.S. Sun, C.Y. Tan, H.X. Liu, Y.B. Jin, Y.Y. Jiang, Exploration of Acridine Scaffold as a Potentially Interesting Scaffold for Discovering Novel Multi-target VEGFR-2 and Src Kinase Inhibitors, *Bioorg. Med. Chem.*, 19 (2011) 3312-3319.
- [45] Y.Q. Li, C.Y. Tan, C.M. Gao, C.L. Zhang, X.D. Luan, X.W. Chen, H.X. Liu, Y.Z. Chen, Y.Y. Jiang, Discovery of Benzimidazole Derivatives as Novel Multi-target EGFR, VEGFR-2 and PDGFR Kinase Inhibitors, *Bioorg. Med. Chem.*, 19 (2011) 4529-4535.
- [46] C. Ding, C.L. Zhang, M.L. Zhang, Y.Z. Chen, C.Y. Tan, Y. Tan, Y.Y. Jiang, Multitarget Inhibitors Derived from Crosstalk Mechanism Involving VEGFR2, *Future Med. Chem.*, 6 (2014) 1771-1789.
- [47] F. Jin, D. Gao, Q. Wu, F. Liu, Y.Z. Chen, C.Y. Tan, Y.Y. Jiang, Exploration of N-(2-aminoethyl)piperidine-4-carboxamide as a Potential Scaffold for Development of VEGFR-2, ERK-2 and Abl-1 Multikinase Inhibitor, *Bioorg. Med. Chem.*, 21 (2013) 5694-5706.
- [48] H.B. Chen, X.B. Zeng, C.M. Gao, P.H. Ming, J.P. Zhang, C.P. Guo, L.Z. Zhou, Y. Lu, L.J. Wang, L.Q. Huang, X.J. He, L. Mei, A New Arylbenzofuran Derivative Functions as an Anti-tumour agent by Inducing DNA Damage and Inhibiting PARP Activity, *Scientific Rep.*, 5 (2015).
- [49] B. Zhang, X. Li, B. Li, C.M. Gao, Y.Y. Jiang, Acridine and Its Derivatives: a Patent Review (2009-2013), *Expert Opin. Ther. Pat.*, 24 (2014) 647-664.
- [50] A.L. Larroque-Lombard, N. Ning, S. Rao, S. Lauwagie, R. Halaoui, L. Coudray, Y. Huang, B.J. Jean-Claude, Biological Effects of AL622, a Molecule Rationally Designed to Release an EGFR and a c-Src Kinase Inhibitor, *Chem. Biol. Drug Design*, 80 (2012) 981-991.
- [51] S.Y. Yang, X.Y. Huang,  $\text{Ca}^{2+}$  Influx Through L-type  $\text{Ca}^{2+}$  Channels Controls The Trailing Tail Contraction in Growth Factor-induced Fibroblast Cell Migration, *J. Biol. Chem.*, 280 (2005) 27130-27137.

- [52] H.K. Kleinman, Preparation of Basement Membrane Components from EHS Tumors, *Curr. Protoc. Cell Biol.*, Chapter 10 (2001) Unit 10 12.
- [53] M.M. Zatz, Culture of Animal-Cells - a Manual of Basic Technique - Freshney,Ri, *Am. Sci.*, 72 (1984) 204-204.

ACCEPTED MANUSCRIPT



Scheme 1

- A series of azaacridine derivatives were rationally designed and synthesized.
- Azaacridine compounds acted as potent EGFR and Src dual inhibitors.
- Compound **13b** could inhibit the activity of EGFR and Src.
- Compound **13b** inhibited the migration of A549 cells.
- Compound **13b** could effectively induce cancer cells apoptosis.

ACCEPTED MANUSCRIPT